Topological analysis of the bonds in incomplete cuboidal $[Mo_3S_4]$ clusters

Marta Feliz,[a] Rosa Llusar,*[a] Juan Andrés,[a] Slawomir Berski[a] and Bernard Silvi[b]

[a] *Departament de Ciències Experimentals, Universitat Jaume I, Box 224, 12080 Castelló, Spain*
[b] *Laboratoire de Chimie Théorique, Université Pierre et Marie Curie, UMR-CNRS 7616, Paris, France*

Received (in London, UK) 21st March 2002, Accepted 23rd April 2002
First published as an Advance Article on the web 31st May 2002

The nature of the bonding interactions within the trinuclear $[Mo_3S_4Cl_3(PH_3)_6]^+$ cluster with an $[M_3X_{13}]$ structural type has been investigated using the present topological theories of the chemical bond. The values of the electron density at the Mo–Mo and Mo–ligand bond critical points (bcps) are small, making a topological description of the bond using the electron density as the scalar function difficult. The characteristics of the different bonds can be better understood using the delocalization index, δ(A, B), or through a topological analysis of the electron localization function (ELF), $\eta(r)$. The delocalization indexes involving the Mo and S centers within the $[Mo_3S_4]$ cluster core are in good agreement with the predominant covalent character of the Mo–Mo and Mo–S bonds. The $[Mo_3S_4]$ unit is unambiguously identified as a chemical entity in the first ELF bifurcation diagram, and futher increasing the $\eta(r)$ value separates the the Mo–S and S valence domains from that of the $[Mo_3]$ core, which further splits into three disynaptic V(Mo, Mo) basins and one trisynaptic V(Mo, Mo, Mo) basin. Calculations of the basin populations and their covariances suggest the existance of a delocalized Mo-(μ_2-S)-Mo bond. Analysis of the orbital contribution to the V(Mo, Mo) and V(Mo, Mo, Mo) basins enables us to establish a relationship between the topological and the MO picture of the bond.

1 Introduction

The field of metal cluster chemistry has emerged as a major area within inorganic chemistry over the past 30 years.[1,2] One determining factor in the development of this area has been the idea that cluster compounds can serve as effective models for homogeneous as well as heterogeneous catalysts. A metal cluster compound has been defined as a group of two or more atoms where direct and substantial metal–metal bonding is present. Although this has proved to be a reasonable working definition, the criterion "direct and substantial metal–metal bonding" has proved to be more ambiguous than originally thought due to the wide range in metal–metal bond distances observed for compounds with the same formal bond order. A preliminary understanding of the bonding in these compounds has arisen from a combination of theoretical ideas derived from molecular orbital theory and the application of spectroscopic techniques such as photoelectron spectroscopy.

For transition metals in their bulk state, maximum binding energies are achieved at the center of the transition series corresponding to half-filling of the "d" and "s" bands. In molecular clusters, the ligands modify the electronic structure configuration of the metals in an attempt to emulate this situation. Therefore, for the earlier transition metals, σ-donor ligands contribute extra electrons, and for the later transition metals, π-acid ligands remove excess electron density. Molybdenum has proved to have a great tendency to form trinuclear clusters under a wide variety of reaction conditions.[3] Among the different structural types encountered for these trinuclear clusters, our interest has been focussed on that designated as $[M_3X_{13}]$ and represented in Fig. 1, this arrangement core can be formulated as $(MX^i_{2/2}X^{iii}_{1/3}X^a_3)_3$, where outer and inner ligands are designated by "a" and "i", respectively. The structure consists of three MX_6 coordinated octahedra, fused together so that each octahedron shares one vertex (X^{iii}) and two edges (X^{iii}–X^i). One alternative description of this structure considers the three metal atoms defining an equilateral triangle, with one capping atom (X^{iii}) above and three bridging atoms (X^i) below the plane described by the metals. Three more ligands on each metal are distributed so as to complete the local octahedra.

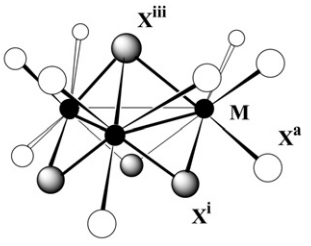

Fig. 1 Structure of the $[M_3X_{13}]$ trimer from shared octahedra.

A simple but widely used scheme for the metal–metal bonding in the $[M_3X_{13}]$ system is that based on the empirical method formulated by Cotton and Haas (CH) for the $[Mo_3O_{13}]$ unit in the early sixties.[4,5] According to this scheme, these trinuclear clusters should be stable when there are six metal "d" electrons available to enter the low energy $1a_1$ and 1e metal cluster orbitals, which correspond to three metal–metal bonding orbitals. Compounds with seven or eight metal electrons may also be stable, since the additional electrons occupy the next highest orbital ($2a_1$), which is approximately M–M non-bonding. This simplified scheme was also supported by Dahl's qualitative orbital analysis model, which predicts the existence of nine cluster orbitals involving metal–metal interactions, among which three are strongly bonding ($1a_1$ and 1e) and one is weakly bonding ($2a_1$), in these incomplete cubane-type clusters.[6] Further studies using the

 DOI: 10.1039/b202907c

non-empirical Fenske–Hall method, which takes into consideration metal–ligand bonding, support the above electronic formulation and, at the same time, show a higher influence of the bridging *versus* the capping atoms on the population of the metal cluster orbitals, $1a_1$ and 1e, while the effect of the terminal ligands upon the populations of the these canonical orbitals is negligible.[7] Fragment calculations on the $[Mo_3(\mu_3\text{-}S)(\mu_2\text{-}Cl)_3Cl_9]^{2-}$ system by Hoffman *et al.*, employing angular overlap model arguments that sequentially include the inner and outer cluster ligands, corroborate the validity of the CH scheme. On the other hand, this work indicates that addition of terminal chloride ligands to the $[Mo_3(\mu_3\text{-}S)(\mu_2\text{-}Cl)_3]$ core lowers the HOMO–LUMO energy gap.[8]

Semiempirical calculations by Wendan and co-workers and Chen *et al.* show extensively delocalized Mo(d)–$S^i(p_\pi)$ bonding, which results in a continuous closed d–p_π system, $Mo_3(\mu_2\text{-}S)_3$, with strong interactions between the localized Mo–(μ_2-S)–Mo three-center-two-electron bonds. This delocalization has been referred to as "quasi-aromaticity".[9–12] This idea has also been supported by Hartree–Fock *ab initio* calculations.[13]

Molecular orbital studies employing Xα density functionals (SCF-Xα-SW and DV-Xα) indicate that changes in the intimate ligand in the central $[Mo_3X_4]$ (X = O, S, Se, Cl) core affect the relative stabilities of different oxidation levels of the metal atoms and that, in the case of clusters with $[Mo_3S_4]$ central units, metal electronic populations different from 6 e^- remain rare.[14–17] On the other hand, changes in the inner ligands, as with peripheral ligands, affect the atomic contributions to the frontier orbitals (HOMO, HOMO-1, LUMO...) and, consequently, the reactivity of the system.

Recently, we have focussed our interest on the topological analysis of the metal–metal bonds. In this paper, we extend our interest to the incomplete cuboidal molecular cluster of formula $[Mo_3S_4Cl_3(PH_3)_6]^+$, with an $[M_3X_{13}]$ structure type. Although qualitative symmetry arguments seem to be valid in most cases, it is clear that extensive mixing between the metals and the core and outer ligands complicate the bonding situation and, as a consequence, a detailed analysis of the interactions must be carried out for a particular system. This paper is organized as follows: the first section provides a conceptual survey of the topological analysis of the electron localization function (ELF). The topological bond principles are applied to the $[Mo_3S_4Cl_3(PH_3)_6]^+$ cluster using the atom-in-molecules (AIM) and the ELF methodologies and the results are also analyzed within the framework of molecular orbital (MO) theory.

2 Topological analysis of the electron localization function

Chemists' intuitive vision of bonding in molecules implicitly assumes a partition of space into adjacent regions corresponding to chemically meaningful entities such as atomic cores, bonds, and lone pairs. The aim of the topological approach to the chemical bond is the determination of such regions and of their boundaries, with the help of rigorous mathematical tools. The theory of dynamical systems is certainly one of the best which can be employed to reach this goal because it is a generalization and a formalization of the techniques used in geography to determine river basins and watersheds. It usually requires the knowledge of a scalar function of the space coordinates where each of its local maxima is associated with a region of space called a basin.[18]

In the case of chemical bonding, the information carried by the local values of the function should be closely related to the pairing of electrons, a cornerstone in all bonding theories. As electrons are half-integer spin particles (fermions), two electrons with identical spins tend to avoid each other more strongly than two electrons with antiparallel spins. This effective Pauli repulsion adds up to the simple electron–electron electrostatic interaction. The number of electrons with the same spin that a given electron has around it within an elementary volume with an arbitrarily defined small charge can be taken as a good measure of the local fermionic behaviour. Becke and Edgecombe's electron localization function (ELF) is derived from this measure of pairing and is confined within the [0,1] interval.[19,20] It tends to 1 where parallel spins are highly improbable (for example, inside a lone pair or a bond region), whereas it is close to 0 near the boundaries of the electronic domains where electrons with parallel spins are compelled to come close to one another.

ELF topological analysis provides a partition of the molecular space in basins, which is consistent with the assumptions of Lewis theory. There are accordingly core and valence basins, labeled C(A) and V(A,B,...), respectively, with A and B being the atoms concerned. The valence basins are characterized by the number of core basins with which they share a boundary. This number is called the synaptic order. This notion of synaptic number introduces a homogeneous nomenclature for the valence basin (monosynaptic, lone pair; disynaptic, two-center bond; trisynaptic, three-center bond...) that accounts for multicenter bonds in a natural fashion.[21] The ELF basins provide a complementary view to the standard valence one. Instead of counting the atoms coordinated to a given nucleus, one is immersed in the basin of interest and counts the bordering cores. Quantitative information can be further extracted by integrating the electron density over these localization basins.[22–24]

3 Computational method

Calculations were performed at the restricted Hartree–Fock (HF) and Becke's hybrid density functional (B3LYP)[25,26] levels with the Gaussian 98 program.[27] The geometry of the model compound $[Mo_3S_4Cl_3(PH_3)_6]^+$ was optimized assuming a C_3 symmetry, in agreement with the observed experimental symmetry. The HF and B3LYP methods were used in conjunction with the standard 3-21G and 3-21G(d, p) basis sets for all atoms and the double-ζ pseudo-orbital basis set LanL2DZ, in which the metal atoms are represented by the relativistic effective core LanL2 potential of Los Alamos.[28] In addition, wavefunctions were also obtained for the optimized geometries at the B3LYP level of theory, combining the Stuttgart group's quasi-relativistic effective core potential and valence split basis sets with different contraction schemes, namely {311111/2211/411}(ECP-VBS1), {31111/411/311/1} (ECP-VBS2), and {31111/411/311/11} (ECP-VBS3) for the molybdenum atoms.[29,30] The even scale rule was applied in the ECP-VBS3 basis set: a single f-polarization function having an exponent α (1.048) was replaced with two functions with exponents α/2 (0.524) and 2α (2.097).[31] The all-electron 6-31G(d, p) and 6-31G++(d, p) basis sets were employed for the remaining atoms.

The ELF and AIM calculations were computed with the TopMod package.[32,33] Isosurfaces were visualized with the program SciAn.[34]

4 Results and discussion

4.1 Geometry optimization for $[Mo_3S_4Cl_3(PH_3)_6]^+$

The $[Mo_3S_4Cl_3(PH_3)_6]^+$ model cluster represented in Fig. 2 belongs to the $[M_3X_{13}]$ structural type, one of the most common structures in early transition metal trinuclear clusters. This compound has been taken as a model for the crystallographically characterized $[Mo_3S_4Cl_3(dmpe)_6]^+$ [dmpe = 1,2-bis(dimethylphosphino)ethane] which crystallizes in the

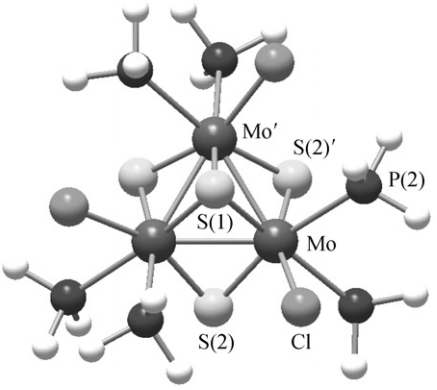

Fig. 2 Structure of the model trimer $[Mo_3S_4Cl_3(PH_3)_6]^+$, with atom numbering scheme.

non-centrosymmetric space group *R*3*C* with a C_3 symmetry; as a consequence, geometry optimization was undertaken assuming this point group symmetry for the molecule.[35] Table 1 presents some of the relevant results regarding geometry optimization for this system, together with the experimental values.

As already observed for other transition metal clusters, the DFT method yields interatomic distances which are much closer to the experimental values than those calculated with the HF methodology. The HF-optimized intermetallic distances are between 0.36 and 0.16 Å longer than the experimental values, whereas deviations provided by DFT calculations are one order of magnitude smaller. This discrepancy is probably due to HF overestimation of the ionic character, which increases the repulsive interaction between metallic centers through an increase in the atomic net charge. It is worth noting that the HF AIM charges on the molybdenum atoms are approximately 0.2 a.u. larger than the corresponding DFT charges computed for the same basis set.

With respect to the geometry optimization criterion, the best results are obtained for the DFT calculations using the all-electron 3-21G(d, p) basis set (AE), in which there is no statistically significant deviation between the optimized and experimental intermetallic bond distances, and with a stardard deviation in the molybdenum first coordination sphere bond distances, namely Mo–S (P or Cl), of 0.013 Å. Calculations carried out with the Stuttgart effective core potential for the molybdenum atoms in conjunction with the 6-31G(d, p) basis set for the remaining atoms (ECP-VBS1, ECP-VBS2, ECP-VBS3) give Mo–Mo bond lengths between 0.036 and 0.008 Å longer than the experimental values. The lower deviation corresponds to the Stuttgart pseudopotential with a valence split {31111/411/311/11} basis for Mo (ECP-VBS3), which gives a standard deviation for the relevant bond distances listed in Table 1 of 0.03 Å. The addition of diffuse funtions to the non-metal atoms does not significantly affect the optimized interatomic distances.

In all calculations, the Mo–(μ_2-S) bond distance *trans* to the phosphorus atom is longer than that *trans* to the halogen, reflecting the larger *trans* influence of the phosphorus atom *versus* chlorine. The most relevant differences between the optimized interatomic distances obtained through B3LYP calculations using the all-electron 3-21G(d, p) basis set (AE) or the Stuttgart effective core pseudopotential for Mo, together with the 6-31G++(d, p) basis for the non-metal atoms, has to do with the Mo–P bond lengths, which are 0.04 Å for P(1) and 0.06 Å for P(2) longer for the pseudopotential case, and with the 3-21G(d, p) results more closely resembling the experimental values. In both cases, the Mo–P(1) distance *trans* to the μ_3-S(1) atom is shorter than the Mo–P(2) bond length *trans* to the μ_2-S(2), as expected based on the longer Mo–μ_3-S(1) distance.

Angles calculated with both AE and ECP for the [Mo(μ_3-S)(μ_2-S)$_3$] cluster core agree within about 0.5 and 0.2° for the 3-21G(d, p) basis set and the ECP-VBS3/6-31G++(d, p) combination, respectively. Larger discrepancies are found in the molybdenum–molybdenum–outer ligand (P, Cl) bond angles, and are calculated to be between 1 to 5°.

4.1 Topological analysis for $[Mo_3S_4Cl_3(PH_3)_6]^+$

4.1.1 Atoms-in-molecules analysis. The quantum theory of atoms in molecules (QTAIM) uses the electron density to assign a molecular structure and the physics of an open system to determine the nature of a bonded interaction.[18] According to this theory, a chemical structure is defined by a network of bond paths or unique lines of maximum electron density that link the nuclei of neighboring atoms in an equilibrium geometry. The presence of a bond path provides an universal indicator of bonding between atoms.[36]

Table 1 Optimized and experimental structure parameters for the $[Mo_3S_4Cl_3(PH_3)_6]^+$ model trimer

	HF		B3LYP					
	LanL2DZ	3-21G(d, p)	LanL2DZ	3-21G(d, p)	ECP-VBS1[a]	ECP-VBS2[a]	ECP-VBS3[b]	Exptl[c]
Distances/Å								
Mo–Mo	3.128	2.929	2.802	2.767	2.802	2.789	2.775	2.766
Mo–S(1)	2.501	2.409	2.449	2.379	2.388	2.382	2.373	2.360
Mo–S(2)	2.628	2.511	2.403	2.355	2.356	2.349	2.340	2.336
Mo–S(2)′	2.227	2.192	2.361	2.303	2.312	2.306	2.300	2.290
Mo–Cl	2.507	2.485	2.508	2.475	2.484	2.477	2.472	2.473
Mo–P(1)	2.645	2.578	2.608	2.545	2.573	2.577	2.589	2.534
Mo–P(2)	2.621	2.598	2.666	2.602	2.643	2.647	2.662	2.605
Angles/°								
Mo′–Mo–S(1)	51.299	52.562	55.110	54.450	54.079	54.164	54.220	54.1
Mo′–Mo–S(2)	91.696	93.912	98.990	98.635	98.369	98.451	98.583	98.4
Mo′–Mo–S(2)′	55.771	56.545	54.682	54.429	53.828	53.911	53.934	54.0
Mo′–Mo–Cl	140.804	140.369	141.367	140.271	141.177	141.304	141.382	136.7
Mo′–Mo–P(1)	141.023	142.338	138.863	140.035	139.312	139.095	138.908	140.9
Mo′–Mo–P(2)	96.831	96.670	93.768	93.996	94.365	94.252	94.278	99.1

[a] Non-metal atoms are represented by the 6-31G(d, p) basis set. [b] Non-metal atoms are represented by the 6-31G++(d, p) basis set. [c] Average bond distances and angles from the crystal structure of $[Mo_3S_4Cl_3(dmpe)_3]^+$; see ref. 35.

The molecular graph obtained for $[Mo_3S_4Cl_3(PH_3)_6]^+$ from the B3LYP calculation is found to reproduce the bond paths corresponding to the Mo–Mo, Mo–Cl, Mo–S, and Mo–P interactions. The charge density along a bond path attains its minimum value at the bond critical point (r_c). The bond critical points (bcp) are the saddle points of the electron density which corresponds to a minimum in the bond path direction and to a maximum in the two perpendicular directions. Large values of $\rho(r_c)$ and negative values of $\nabla^2\rho(r_c)$ for bonds between main groups elements are associated with shared interactions, p. e. covalent bonds, while small values of $\rho(r_c)$ and positive $\nabla^2\rho(r_c)$ values correspond to closed-shell interactions, which include ionic and dative bonds. In the case of interactions between transition metals or transition metals and a ligand the bond critical point characteristics are different, with $\rho(r_c)$ being small and $\nabla^2\rho(r_c) > 0$.[37,38] The values of the electron density at Mo–Mo and Mo–ligand (S, P or Cl) at the bcp are small, in agreement with previous studies on transition metal complexes.[37,39] On the other hand, the Laplacian is positive for all critical points, with the exception of that of the Mo–P pair. This last result is unusual because all transition metal–ligand bonds reported to date, whether they belong to the covalent, dative, or ionic type, have $\nabla^2\rho(r_c) > 0$. The low value of $\nabla^2\rho(r_c)$ for Mo–Mo is consistent with the presence of a metal–metal bond.

The AIM theory provides a definition of atomic charges that is completely different from any other orbital-based population analysis. Atomic charges are obtained by integration of the electron density within the atomic basins and adding the nuclear charge. Based on this, the molybdenum atoms bear a partial charge of +1.13 elementary charges, the sulfur atoms one of −0.54 e^-, and the chlorine and phosphorus atoms −0.55 and +0.04 e^-, respectively. Except for the phosphorus atom, the topological charges are much smaller than the formal charges, namely Mo(+4), S(−2), and Cl (−1). The calculated topological charges are consistent with a partly ionic character for the Mo–S (27% ionic) and Mo–Cl (55% ionic) bonds, and with a dative character for the Mo–P interaction.

The nature of the different bonds within the $[Mo_3S_4Cl_3(PH_3)_6]^+$ complex can be better understood by considering the delocalization index.[40] The delocalization index, δ(A, B) is a measure of the number of electrons shared or exchanged between atoms A and B. Large values for δ(A, B) are indicative of electron-shared interactions (*i.e.* covalent), while low δ(A, B) values characterize closed-shell interactions (*i.e.* ionic or hydrogen bond). Ángyán, Loos, and Mayer have defined topological bond orders as twice the pair covariance, that, at our level of theory, yields values identical to those obtained using δ(A, B).[41] However, Bader *et al.* have pointed out that it is not always appropriate to identify the delocalization index, δ(A, B), with a bond order, since a non-vanishing delocalization index exits between every pair of atoms in a molecule.[42] δ(Mo, Mo) has been calculated to be 0.58, this value is approximately one half that calculated for the Rh_2(formamidinate)$_4$ dimer, with an Rh–Rh topological bond order of 1.008, in spite of the fact that a formal metal–metal bond order of one is assigned to both complexes.[43] The delocalization indexes involving the Mo and S centers within the $[Mo_3S_4]$ cluster core are δ[Mo, μ_3-S(1)] = 0.88, δ[Mo, μ_2-S(2)] = 1.16, and δ[Mo, μ_2-S(2′)] = 1.06, in good agreement with the predominantly covalent character of the Mo–S bonds. Longer metal–sulfur distances correspond to lower values for the delocalization indexes. The δ(Mo, ligand) values for the outer ligands, phosphine and chloride, are δ(Mo, Cl) = 0.66, and δ(Mo, P) = 0.54 and 0.48 for P(1) and P(2), respectively. These values confirm the partly ionic character of the Mo–Cl bond and the dative nature of the Mo–P interaction.

4.1.2 ELF analysis. The concept of localization domain as the molecular volume bounded by one external and eventually internal closed ELF isosurface, $\eta(r)$ = constant, enables the definition of chemical units within a system. A localization domain that contains more than one attractor is called reducible. Upon increasing the value $\eta(r)$ defining the bonding isosurface, a reducible domain splits into several domains, each containing less attractors (core and/or valence) than the parent domain. The reduction of localization domains obtained by increasing the $\eta(r)$ value enables tree diagrams that reflect the hierarchy of the basins and which are characteristic of a given chemical system to be built. In addition, chemical units are unambiguously defined as the set of basins of the last irreducible domain. Scheme 1 shows the bifurcation tree diagram for $[Mo_3S_4Cl_3(PH_3)_6]^+$.

The complex $[Mo_3S_4Cl_3(PH_3)_6]^+$ shows a first bifurcation at $\eta(r) = 0.15$ between the core domains of the light atoms and the remaining reducible domain encompassing all the valence attractors and the Mo core attractors. At larger values of ELF [$\eta(r) \cong 0.25$] this domain splits into six phosphine (PH_3) valence domains, three chlorine valence domains and an $[Mo_3S_4]$ domain. The next bifurcation takes place at $\eta(r) \cong 0.35$ and separates the sulfur valence domains from those of the $[Mo_3]$ core. As a consequence, three different chemical units are identified first: the phosphine and chloride ligands on one side and the $[Mo_3(\mu_3\text{-}S)(\mu_2\text{-}S)_3]$ cluster core on the other side. Further increasing the $\eta(r)$ value yields a separation of the Mo–S and S valence domains from that of the $[Mo_3]$, which further splits into three disynaptic V(Mo, Mo) and one trisynaptic V(Mo, Mo, Mo) basins.

The bifurcation diagram and basin populations are basically independent of the level of calculation. Table 2 lists the basin populations (N) and their covariance and atomic basin contributions calculated at the 3-21G(d, p) and ECP-VBS3 levels. The only noticeable differences in populations between the AE and ECP calculations are in the V(Cl) and V(Mo, Cl)

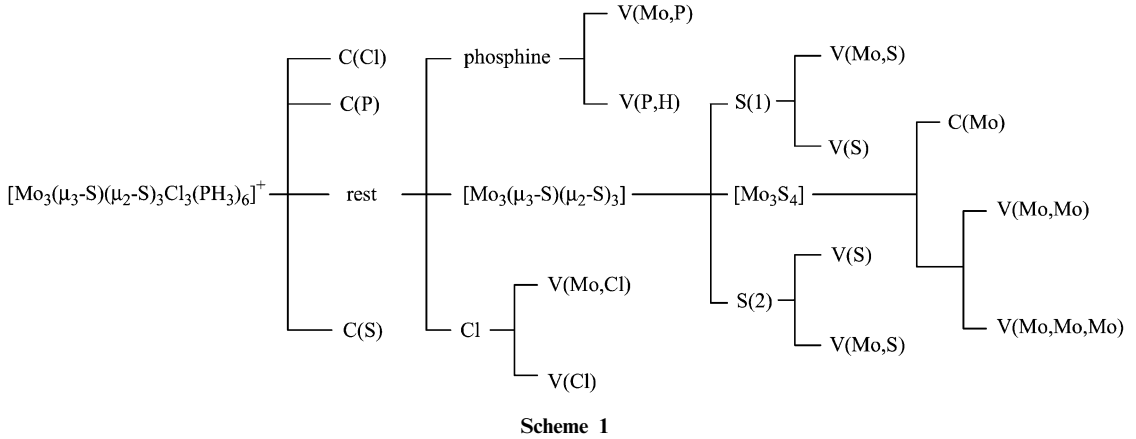

Scheme 1

Table 2 Average valence population, covariance, and atomic basin contribution (e^-) for the $[Mo_3S_4Cl_3(PH_3)_6]^+$ model trimer[a]

	3-21G(d, p)	ECP-VBS3		
Basin	*N*	*N*	σ^2	Atomic contribution analysis
V(Mo–Mo-Mo)	0.34	0.17	0.16	Mo, 0.05 × 3
V(Mo–Mo)	0.23	0.36	0.33	Mo, 0.18 × 2
V[Mo–S(1)]	1.40	1.48	1.00	Mo, 0.20; S(1), 1.27
V[Mo–S(2)]	1.63	1.08	0.78	Mo, 0.19; S(2), 0.89
V[Mo–S(2)′]	1.59	1.50	1.02	Mo, 0.24; S(3), 1.25
V(Mo–Cl)	—	0.56	0.46	Mo, 0.07; Cl, 0.49
V[Mo–P(1)]	1.96	1.93	1.04	Mo, 0.19; P(1), 1.74
V[Mo–P(2)]	1.96	1.95	1.03	Mo, 0.17; P(2), 1.77
C(Mo)	39.35	39.22	2.55	Mo, 39.22
V[S(1)]	2.79	2.70	1.28	S(1), 2.69
V[S(2)]	3.72	4.45	1.86	Mo, 0.09; S(2), 4.33
V(Cl)	4.14	3.83	1.59	Mo, 0.02; Cl, 3.80
V(Cl)	3.36	3.23	1.46	Mo, 0.02; Cl, 3.20

[a] All the calculations were performed with the B3LYP functional at the level shown.

basins on one side and in the V[S(2)] and V[Mo–S(2)] basins on the other side. In the case of the former ligand, the AE calculation gives two V(Cl) monosynaptic basins, whereas an additional disynaptic V(Cl, Mo) basin has been identified with ECP. These apparent inconsistencies can be attributed to the flatness of the attractor associated with this V(Mo, Cl) basin. We call this attractor flat because the ELF value at this point, $\eta(r) = 0.838$, is very close to that calculated at the index 1 saddle point, $\eta(r) = 0.834$, located on the separatrice between this and the two V(Cl) basins. In fact, the chemically meaningful entity is either the set of the two V(Cl) basins, with a total population of 7.5 e^-, for the AE calculation, or that formed by these two together with the V(Mo–Cl) basin for the ECP calculation. The sum of the three basin populations in this last case equals 7.62 e^-, which is very close to the AE value, as expected. In the same manner, the shallow separation between the V[Mo–S(2)] and the V[S(2)] basins explains the discrepancies in the populations calculated at the two levels.

We will first start by analysing the bonds to the outer ligands, phosphine and chloride. The topology of the PH_3 ligand in the cluster is very similar to that of the free phosphine, except that the monosynaptic basin V(P) with a population of 2.1 e^- transforms upon coordination to the Mo atom into a disynaptic V(Mo, P) basin with a population of 1.94 e^-, corresponding to the formation of a dative P → Mo bond where approximately 90% of the atomic basins contribution is due to phosphorus. The decrease in population upon coordination can be attributed to a weak charge transfer from the phosphorus towards the hydrogens. The most important contributions to the large variance of the V(Mo–P) basin population arises from the V(P-H) (48%), C(Mo) (17%), and C(P) (13%) basins.

Regarding the bond to chlorine, as previously mentioned, there are two types of basins around the Cl atom: two monosynaptic V(Cl) basins with a total population of 7.06 e^- and a disynaptic V(Mo, Cl) basin with 0.56 e^-. It is worth nothing that the sum of the populations of these three basins is close to the chlorine AIM population (7.62 *versus* 7.55 e^-). The existence of a disynaptic Mo–Cl basin with a low population is compatible with a partly covalent bond where 88% of the basin population is located at the chlorine atomic basin, indicating a high polarity for this bond. The V(Mo, Cl) population has large variance (*i.e.* $\sigma^2 = 0.46$) which mostly comes from the interaction of this basin with the two monosynaptic V(Cl) basins, in agreement with the flatness of the V(Cl, Mo) attractor.

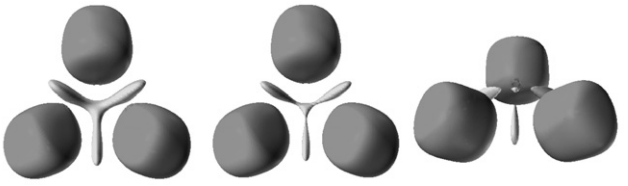

Fig. 3 Detail of the Mo_3 subsystem in $[Mo_3S_4Cl_3(PH_3)_6]^+$, sharing the Mo cores and the valence Mo–Mo basins. From left to right, the isosurfaces are 0.34, 0.36, and 0.365.

Within the $[Mo_3(\mu_3\text{-}S)(\mu_2\text{-}S)_3]$ valence domain, the trihapto-coordinated sulfur atom, S(1), is surrounded by three V[Mo,S(1)] disynaptic basins assigned to the three covalent Mo–S(1) bonds, with a population of 1.48 e^- each, and a monosynaptic basin populated by 2.7 e^-. On the other hand, the basins involving the metal bonds to the three bridging sulfur ligands, Mo–S(2), have populations of 1.08 and 1.5 e^- due to the asymmetry in the sulfur coordination: *trans* to the P or to the Cl atom. In these particular cases, differences in basin population have no chemical meaning due to the difficulties in reducing the V[S(2)] valence domains, which possess a global population of 7.03 e^-, into two Mo–S and one monosynaptic basins containing the two sulfur lone pairs, as previously pointed out. Most of the atomic contributions to the Mo–S basins, 86% for Mo–S(1) and approximately 83% for Mo–S(2) basins, comes from sulfur, supporting the partial ionic character of the bond.

The $[Mo_3]$ cluster unit behaves as a specific entity where the bonding arises from the presence of a three-center bond associated with a group of basins involving three disynaptic V(Mo, Mo) and one trisynaptic V(Mo, Mo, Mo) basins. Fig. 3 shows the valence $[Mo_3]$ superbasin and its separation into the previously mentioned four domains. Because this separation takes place in a very narrow ELF range, the chemically meaningful entity is the four basins group as a whole rather than the individual domains.

The total population of this $[Mo_3]$ valence superbasin is 1.25 e^-, a large value as compared to the value of 0.68 e^- calculated for the disynaptic intermetallic basin in the $[Mo_2(formamidinate)_4]$ quadruply bonded dimer. In the $[M_2(formamidinate)_4]$ dimers, where M = second row transition metal, the metal–metal bond is considered to be due to the fluctuation of electrons within core areas.[43] However, this is not the case for the $[Mo_3]$ unit under consideration, where the Mo–Mo′ core covariance is small, B(Mo, Mo′) = 0.14 e^-, in spite of the rather large value of the Mo core population covariance, $\sigma^2 = 2.55$ a.u. The main contributors to this variance are the bridging sulfur lone pair V[S(2)] basins with 0.2 e^- each, and the disynaptic V[Mo,S(2)] basins with 0.4 (*ca.* 2 × 0.2) e^-. This is in agreement with delocalized Mo–μ_2-S(2)–Mo bonding, as suggested by Li *et al.*[13] and previously pointed out in the introduction. However, these authors relate this delocalization to the existence of a 3c-2e^- bond and refer to this situation as "pseudo-aromaticity". A trisynaptic basin is the topological signature of a true three-center bond, such as it exists in diborane, $Al_2(CH_3)_6$, and in molecules containing tetracoordinated planar carbon.[44,45] In the present complex, there is no V(Mo, S, Mo) trisynaptic basin and therefore a 3c-2e^- bond cannot be invoked.

The molybdenum core population of 39.22 e^- corresponds approximately to Mo^{3+} rather than to Mo^{4+}, which is the formal oxidation state assigned to Mo in this system. This situation is normal when calculating metal core population in transition metal complexes.[43]

4.1.3 MO *versus* topological analysis. The simplified MO picture of the bond in trinuclear $[Mo_3X_{13}]$ clusters assigns the three M–M bonds to the occupation of three molecular

orbitals of symmetry a_1 (HOMO-1) and e (HOMO). Although this is the essence of most of the calculations carried out in different trinuclear clusters of this structural type, the situation gets more complicated due to the interaction of the metal with the ligand orbitals. *Ab initio* studies carried out by Cotton *et al.* on $[Mo_3]$ clusters show that the energy levels, and hence the electron count, depends on the detailed nature of the atoms in the $[M_3X_4]$ core and the outer ligands. For example, *ab initio* calculations on the cluster $[Mo_3S_4Cl_6(PH_3)_3]^{2-}$ show that the HOMO possesses a_1 symmetry and mainly Mo–P bonding character. In this cluster, the metal–metal character represented by the $1a_1$ orbital is distributed over several orbitals of lower energy.[14]

The energy level ordering calculated from the combination ECP-VBS3/6-31G++(d, p) for the top part of the diagram ($1a_1 < 1e < 2a_1$) agrees with the CH scheme. In order to evaluate the metallic character of these orbitals, we have calculated their atomic contributions based on the atomic definition of the AIM theory. The "HOMO"(1e) and "HOMO-1" ($1a_1$) have 39 and 44% Mo character, respectively, with important contributions from the chlorine atoms (36% for the "HOMO" and 25% for the "HOMO-1" orbitals) and the bridging (15% for "HOMO" and 8.5% for "HOMO-1") and capping (7.5% for "HOMO" and 13.5% for "HOMO-1") sulfurs. Inspection of the contour diagrams of these orbitals shows their M–M and M–S bonding character. The metal contribution to the "HOMO-2" orbital is only 8.5% and the main atomic contributions to this orbital comes from the bridging sulfurs (38.5%) and the Cl atoms (38%). The large energy gap between the "HOMO" and "LUMO" orbitals, 3.2 eV, strongly disfavours a seven or eight-electron population for the $[Mo_3S_4]$ core in the $[Mo_3S_4Cl_3(PH_3)_6]^+$ trimer. To date, only two examples of trinuclear $[Mo_3S_4]$ clusters with 7 metal electrons have been reported, namely $[Mo_3S_4Cl_3(dppe)_3(PEt_3)]$ and $[Mo_3S_4Cp^*_3]$.[16,17]

A different perspective to relate the MO picture of the bond with the topological one provide by the analysis of the ELF function is to calculate the orbital contributions to the valence metal basin associated with the metallic bond within the $[Mo_3]$ triangle, that is the three disynaptic V(Mo, Mo) and the trisynaptic V(Mo, Mo, Mo) basins. The orbital contributions to these basins are spread over a large number of molecular orbitals. However, the larger contributions to the V(Mo, Mo) basins come from the "HOMO" (1e) and "HOMO-1" orbitals ($1a_1$) at 17%. Contributions from other orbitals are less than 5%. The major contributions of the "HOMO" orbital are to the molybdenum core basins, followed by the V[S(2)] and V(Cl) valence basins.

The $1a_1$ ("HOMO-1") orbital contributes 0.03 e^- to the trisynaptic V(Mo, Mo, Mo) basin, which has a population of 0.17 e^-, and, consequently, this accounts for 18% of the contribution. Again, the orbital contribution to this basin is spread over a large number of orbitals, but with values always lower than 12%. The more significative contributions of the "HOMO-1" orbital are to the C(Mo) basins, followed by the chlorine and capping and bridging sulfur valence basins.

Conclusions

A combined analysis of the topological properties of the electron density and the electron localization function in the incomplete cuboidal cluster complex $[Mo_3S_4Cl_3(PH_3)_6]^+$ provides an alternative interpretation of the bond to the one provide by the simplified Cotton and Haas molecular orbital scheme. In this MO picture, six metal "d" electrons enter the low energy $1a_1$ (HOMO-1) and 1e (HOMO) metal cluster orbitals, which correspond to three metal–metal bonding orbitals. The topological analysis provide a view of the bond based on a local description that, in contrast to other population analyses, is independent of the partition system employed. The atomic populations, together with the delocalization indexes between the Mo–Mo, Mo–S, and Mo–outer ligand atoms provided by the AIM theory, are a clear indication of the nature of the interaction, covalent for Mo–Mo and Mo–S, partly ionic for Mo–Cl and dative for Mo–P. The bifurcation diagram obtained when increasing the ELF function values clearly identifies the $[Mo_3(\mu_3\text{-}S)(\mu_2\text{-}S)_3]$ unit as a chemical entity, while the metal–metal bond within the $[Mo_3]$ triangle is characterized by three disynaptic V(Mo, Mo) and a trisynaptic V(Mo, Mo, Mo) basins, with a total population of 1.25 electrons. This population is approximately twice that calculated for the quadruply bonded $[Mo_2(formamidinate)_4]$ dimer. The fluctuation of electrons within the core areas is small in comparison with the values calculated for the metal–metal-bonded $[M_2(formamidinate)_4]$ dimers, where M = second row transition metal. While in this last case the metal–metal bond has been associated to fluctuations within the core areas, the metal–metal bond in the $[Mo_3S_4Cl_3(PH_3)_6]^+$ cluster is associated with the presence of a direct Mo–Mo bond, deduced from the presence of metal valence basins, and with delocalized Mo–(μ_2-S)–Mo bond interactions inferred from the covariance analysis of the basin population.

Acknowledgements

Financial support from Ministerio de Educación y Ciencia (DGESIC, research projects PB98-1044 and 1FD1997-1765-C03-02) and Fundació Caixa Castelló-UJI (research project P1·1B2001-07) is gratefully acknowledged. B. S. thanks the Iberdrola Foundation for financing his stay as a visiting professor at the Universitat Jaume I. S. B. thanks the Fundació Caixa Castelló-UJI for financing his stay as a postdoctoral fellow at the Universitat Jaume I.

References

1 D. M. P. Mingos and D. J. Wales, in *Introduction to Cluster Chemistry*, ed. R. N. Grimes, Prentice-Hall, Englewood Cliffs, NJ, 1990, ch. 1.
2 P. Braunstein, L. A. Oro and P. R. Raithby, *Metal Clusters in Chemistry*, Wiley-VCH, Weinheim, 1999.
3 A. Müller, R. Jostes and F. A. Cotton, *Angew. Chem., Int. Ed. Engl.*, 1980, **19**, 875.
4 F. A. Cotton and T. E. Haas, *Inorg. Chem.*, 1964, **3**, 10.
5 F. A. Cotton and T. E. Haas, *Inorg. Chem.*, 1964, **3**, 1217.
6 P. J. Vergamini, H. Vahrenkamp and L. F. Dahl, *J. Am. Chem. Soc.*, 1971, 6327.
7 B. E. Bursten, F. A. Cotton, M. B. Hall and R. C. Najjar, *Inorg. Chem.*, 1982, **21**, 302.
8 Y. Jiang, A. Tang, R. Hoffmann, J. Huang and J. Lu, *Organometallics*, 1985, **4**, 27.
9 C. Wendan, Z. Qianer, H. Jinshun and L. Jiaxi, *Polyhedron*, 1989, **8**, 2785.
10 C. Wendan, Z. Qianer, H. Jinshun and L. Jiaxi, *Polyhedron*, 1990, **9**, 1625.
11 Z. Chen, J. Lu, C. Liu and Q. Zhang, *Polyhedron*, 1991, **10**, 2799.
12 C. Wendan, G. Guocong, J. Jinshun and L. Jiaxi, *Polyhedron*, 1995, **14**, 3649.
13 J. Li, C. Liu and J. Lu, *Polyhedron*, 1994, **13**, 1841.
14 F. A. Cotton and X. Feng, *Inorg. Chem.*, 1991, **30**, 3666.
15 G. Sakane, T. Shibahara and H. Adachi, *J. Cluster Sci.*, 1995, **6**, 503.
16 R. E. Cramer, K. Yamada, H. Kawaguchi and K. Tatsumi, *Inorg. Chem.*, 1996, **35**, 1743.
17 J. Mizutani, H. Imoto and T. Saito, *J. Cluster Sci.*, 1995, **6**, 523.
18 R. F. W. Bader, *Atoms in Molecules: A Quantum Theory*, Oxford University Press, London, 1990.
19 A. D. Becke and K. E. Edgecombe, *J. Chem. Phys.*, 1990, **90**, 5397.
20 B. Silvi and A. Savin, *Nature*, 1994, **371**, 683.
21 A. Savin, B. Silvi and F. Colonna, *Can. J. Chem.*, 1996, **74**, 1088.
22 M. Kohout and A. Savin, *Int. J. Quantum Chem.*, 1996, **60**, 875.

23 U. Häussermann, S. Wengert, P. Hofmann, A. Savin, O. Jepsen and R. Nesper, *Angew. Chem., Int. Ed. Engl.*, 1994, **33**, 2069.
24 R. Llusar, A. Beltrán, J. Andrés, S. Noury and S. Silvi, *J. Comput. Chem.*, 1999, **20**, 1517.
25 A. D. Becke *J. Chem. Phys.*, 1993, **98**, 5648.
26 C. Lee, Y. Yang and R. G. Parr, *Phys. Rev. B*, 1988, **37**, 785.
27 M. J. Frisch, G. W. Trucks, H. B. Schlegel, G. E. Scuseria, M. A. Robb, J. R. Cheeseman, V. G. Zakrzewski, J. A. Montgomery Jr., R. E. Stratmann, J. C. Burant, S. Dapprich, J. M. Millam, A. D. Daniels, K. N. Kudin, M. C. Strain, O. Farkas, J. Tomasi, V. Barone, M. Cossi, R. Cammi, B. Mennucci, C. Pomelli, C. Adamo, S. Clifford, J. Ochterski, G. A. Petersson, P. Y. Ayala, Q. Cui, K. Morokuma, D. K. Malick, A. D. Rabuck, K. Raghavachari, J. B. Foresman, J. Cioslowski, J. V. Ortiz, A. G. Baboul, B. B. Stefanov, G. Liu, A. Liashenko, P. Piskorz, I. Komaromi, R. Gomperts, R. L. Martin, D. J. Fox, T. Keith, M. A. Al-Laham, C. Y. Peng, A. Nanayakkara, C. Gonzalez, M. Challacombe, P. M. W. Gill, B. Johnson, W. Chen, M. W. Wong, J. L. Andres, C. Gonzalez, M. Head-Gordon, E. S. Replogle and J. A. Pople, Gaussian 98, rev. A7, Gaussian Inc., Pittsburgh, PA, USA, 1998.
28 P. J. Hay and R. Wadt, *J. Chem. Phys.*, 1985, **82**, 270.
29 D. Andrae, U. Haeussermann, M. Dolg, H. Stoll and H. Preuss, *Theor. Chim. Acta*, 1990, **77**, 123.
30 F. Weigend, M. Häser, H. Patzelt and R. Ahlrichs, *Chem. Phys. Lett.*, 1998, **294**, 143.
31 R. Raffenetti *J. Chem. Phys.*, 1973, **58**, 4452.
32 S. Noury, X. Krokidis, F. Fuster and B. Silvi, TopMod Package, Université Pierre et Marie Curie, Paris, France, 1997.
33 S. Noury, X. Krokidis, F. Fuster and B. Silvi, *Comput. Chem.*, 1999, **23**, 597.
34 E. Pepke, J. Murray, J. Lyons and T.-Z. Hwu, SciAn, Scientific Visualization and Animation Program, Supercomputer Computations Research Institute, Tallahassee, FL, USA, 1993.
35 F. A. Cotton and R. Llusar, *Polyhedron*, 1987, **6**, 1741.
36 R. F. W. Bader *J. Phys. Chem. A*, 1998, **102**, 7314.
37 R. Bianchi, G. Gervasio and D. Marabello, *Inorg. Chem.*, 2000, **39**, 2360.
38 R. Bianchi, G. Gervasio and D. Marabello, *Chem. Commun.*, 1998, 1535.
39 R. F. W. Bader and C. F. Matta, *Inorg. Chem.*, 2001, **40**, 5603.
40 X. Fradera, M. A. Austen and R. F. W. Bader, *J. Phys. Chem. A*, 1998, **103**, 304.
41 J. G. Ángyán, M. Loos and I. Mayer, *J. Phys. Chem.*, 1994, **98**, 5244.
42 J. M. Molina, J. A. Dobado, G. L. Heard, R. F. W. Bader and M. R. Sundberg, *Theor. Chem. Acc.*, 2001, **105**, 365.
43 R. Llusar, A. Beltrán, J. Andrés, F. Fuster and B. Silvi, *J. Phys. Chem. A*, 2001, **105**, 9460.
44 B. Silvi *J. Mol. Struct.*, in press.
45 R. Choukroun, B. Donnadieu, J. S. Zhao, P. Cassoux, C. Lepetit and B. Silvi, *Organometallics*, 2000, **19**, 1901.